Fluorine-18-FPCT: A PET Radiotracer for Imaging Dopamine Transporters

Mark M. Goodman, Robert Keil, Timothy M. Shoup, Dennis Eshima, Lorie Eshima, Clinton Kilts, John Votaw, Vernon M. Camp, Delicia Votaw, Elizabeth Smith, Mei-Ping Kung, Eugene Malveaux, Ray Watts, Michael Huerkamp, Ding Wu, Ernest Garcia and John M. Hoffman

Emory Center for Positron Emission Tomography and Department of Neurology, Emory University, Atlanta, Georgia; Department of Radiology, University of Pennsylvania, Philadelphia, Pennsylvania

Fluorine-18-labeled 2β-carbomethoxy-3β-(4-chlorophenyl)-8-(-3-fluoropropyl)nortropane (FPCT) has been synthesized as a new dopamine transporter imaging agent. **Methods:** Fluorine-18 was introduced into 2β-carbomethoxy-3β-(4-chlorophenyl)-8-[-3-fluoropropyl) nortropane by preparation of 1-[^{18}F]fluoro-3-iodopropane followed by alkylation of 2β-carbomethoxy-3β-(4-chlorophenyl)nortropane. **Results:** Tissue distribution studies in rats with [^{18}F]FPCT showed high striatal uptake (0.70% dose/g at 60 min; 0.38% dose/g at 120 min) and good striatal-to-cerebellum ratios (5.5 at 60 min; 6.2 at 120 min). Imaging studies in rhesus monkeys (n = 2) with [^{18}F]FPCT showed high uptake and retention in the putamen (P) (P = 0.03%–0.12% dose/g; at 115 min) and good putamen-to-cerebellum ratios of 3.40–3.43 at 115 min. Plasma metabolites were analyzed in rhesus monkeys (n = 2) by ether extraction and HPLC. The radioactivity in the ether-extractable fraction displayed a single peak that corresponded on HPLC to unmetabolized authentic FPCT. **Conclusion:** These results suggest that [^{18}F]FPCT is an excellent candidate for PET imaging of dopamine transporters.

Key Words: fluorine-18-FPCT; dopamine transporter; fluorotropane; cocaine

J Nucl Med 1997; 38:119–126

Dopamine transporters reside on the membrane of the nerve terminals of the presynaptic mesolimbic dopaminergic neurons. The dopamine transporter serves to remove dopamine from the synapse that regulates central nervous system (CNS) dopamine neurotransmission. Inhibition of the reuptake of dopamine at the transporter and a decrease in transporter density in the striatum has been associated with cocaine addiction (*1*) and Parkinson's disease (*2*), respectively. The neurochemical mechanism responsible for cocaine's reinforcing properties has been hypothesized to involve the binding of (−)-cocaine to the dopamine transporter. Cocaine's inhibition of dopamine removal from the synapse results in an increase in dopamine neurotransmission that produces the euphoric feeling believed to be responsible for cocaine addiction. Regional dopamine receptor density measurements in postmortem brain samples (*3*) and in vivo measurements of dopamine synthesis by PET (*4*) from patients with Parkinson's disease have shown that this disorder is associated with a 60%–80% decrease in the synthesis and neurotransmission of dopamine. In addition to the degeneration of dopamine neurons in the substantia nigra and striatum, recent reports have shown that Parkinson's patients also suffer a corresponding loss of dopamine transporters (*5*).

Because of the crucial role the dopamine transporter plays in the etiology of cocaine addiction and Parkinson's disease, a number of dopamine transporter ligands have been radiolabeled and evaluated for the measurement of presynaptic dopamine transporter sites by emission tomography. Fowler et al. reported on the evaluation of [N-methyl [^{11}C]-(−)-cocaine analogs (*6–9*) in nonhuman primates and humans to measure the time course of cocaine uptake and release at the transporter. These agents do not appear to be attractive candidates for quantifying dopamine transporter sites by PET because they suffer rapid dissociation ($t_{1/2}$=25 min) from the dopamine transporter binding site. The release of [N-methyl^{11}C]-(−)-cocaine analogs from the transporter could result from metabolism of a labile function such as the 8-methyl, 2β-carbomethoxy and 3β-benzoyl groups. Nontropane dopamine transporter ligands have also been labeled with ^{11}C and ^{18}F as potential PET CNS dopamine transporter imaging agents. Imaging studies with [^{11}C]nomifensine in nonhuman and human primates and [^{18}F]GBR 13119 in nonhuman primates have been reported (*10–13*). The imaging data for these ligands appear to show affinity and nonspecific binding only slightly better than those measured with radiolabeled (−)-cocaine. Recently, a series of high-affinity radiolabeled (−)-cocaine analogs have been developed in which the 3β-(benzoyl) group was replaced by more metabolically resistant 3β-(4-substituted-phenyl) groups to overcome rapid dissociation from the dopamine transporter (*14*). These potential dopamine transporter imaging agents include [^{11}C]2β-carbomethoxy-3β-(4-fluorophenyl)tropane (^{11}C-WIN 35,428) (*15–17*), [^{11}C]2β-carbomethoxy-3β-(4-iodophenyl)tropane ([^{11}C]CIT/RTI-55) (*18*) and [^{123}I]2β-carbomethoxy-3β-(4-iodophenyl)tropane ([^{123}I]CIT/RTI-55) (*19–22*). The ^{11}C-labeled 4-fluoro and 4-iodo and the ^{123}I-labeled 4-iodo derivatives showed pronounced striatal uptake in nonhuman primates and humans.

More recently, we have developed [^{123}I] 8-[(E)-3-iodopropen-1-yl]-2β-carbomethoxy-3β-(4-chlorophenyl)nortropane (IPT) as a CNS dopamine transporter SPECT imaging agent (*23*). Iodine-123 was stabilized by attachment as an (E)-3-iodopropen-1-yl substituent at the 8-nitrogen position of 2β-carbomethoxy-3β-(4-chlorophenyl)tropane (CCT). Iodine-123-IPT showed very high uptake in the dopamine transporter-rich striatal tissue with low uptake in the hypothalamus/midbrain, a region with high densities of serotonin transporter sites, and the dopamine transporter-poor cerebellum in rats. Excellent SPECT images of the striatum have been obtained with [^{123}I]IPT in nonhuman primates (*25*). Desirable properties accompanying high striatal uptake of [^{123}I]IPT was rapid peak uptake (25 ± 13 min) followed by gradual clearance and nonvisualization of the hypothalamus/midbrain. These studies have shown that bulk tolerance exists at the 8-position of CCT and that 8-alkenyl substitution does not interfere with high-selective in vivo striatal uptake and suggests that [^{18}F]8-[3-fluoropropyl]-2β- carbomethoxy-3β-(4-chlorophenyl)nortropane ([^{18}F]FPCT) and [^{18}F]8-[2-fluoroethyl]-2β-carbomethoxy-3β-(4-chlorophenyl)nortropane ([^{18}F]FECT) may be attractive candidates for quantifying dopamine transporter

Received Sept. 15, 1995; revision accepted May 16, 1996.

For correspondence or reprints contact: Mark M. Goodman, PhD, Emory University, Dept. of Radiology, 1364 Clifton Rd., NE, Atlanta, GA 30322.

sites by PET. The very short 20-min half-lives of ^{11}C (^{11}C-WIN 35,428) and ([^{11}C]CIT/RTI-55) may not allow ample time for measuring the entry and longitudinal selective regional uptake of the radioligand and analysis of the presence of radiolabeled metabolites that are crucial in receptor imaging and tracer kinetic modeling. Fluorine-18 is a more attractive PET radionuclide for radiolabeling because its 110-min half-life allows sufficient time (3 × 110 min) for incorporation into the tracer molecule and for purification of the final product suitable for human administration.

Second, ^{18}F can be prepared in curie quantities as a fluoride ion for incorporation into the tracer molecule in high, theoretical 1.7 Ci/nmole, specific activity by no-carrier-added nucleophilic substitution reactions. Fluorine-18 is also the lowest energy positron emitter (0.635 MeV, 97% abundant, 2.4-mm positron range) that affords the highest resolution images. Finally, the 110-min half-life allows ample time for measuring the entry and selective regional uptake of the radioligand and analysis of the presence of radiolabeled metabolites.

The goals of the present study were to characterize the in vitro properties of FPCT and FECT, develop a radiosynthesis and evaluate the in vivo distribution of the most potent ligand in rats and nonhuman primates.

MATERIALS AND METHODS

All chemicals and solvents were analytical grade and were used without further purification unless otherwise stated. The [^{18}F] fluoride was produced at Emory University with a Seimens RDS 112 11 MeV negative-ion cyclotron by the $^{18}O(p, n)^{18}F$ reaction using [^{18}O]H_2O (95%). (−)-Anhydroecognine methyl ester was prepared according to literature procedures (*23*). Thin-layer chromatography (TLC) analyses were performed using 250-μm thick layers of G PF-254 silica gel adsorbed on aluminum plates. The proton and carbon nuclear magnetic resonance (NMR) spectra (Appendix) were obtained at 300 and 75 MHz with a GE-300 instrument. Both low- and high-resolution mass spectra (Appendix) were obtained at the Emory Center for Mass Spectroscopy. Elemental analyses were performed by Atlantic Microlab, Inc. (Norcross, GA) and were within 0.3% of the calculated values.

Chemistry

FPCT (4). A solution of 25 mg (0.095 mmol) of 2β-carbomethoxy-3β-(4-chlorophenyl)nortropane in 5 ml of CH_2Cl_2 and 0.1 ml DMF was treated with 50 ml of Et_3N and 130 mg (1.0 mmole) of 3-fluoro-1-bromopropane and stirred for 16 hr. The solution was diluted with 10 ml CH_2Cl_2, washed with 1 N NaOH, dried with sodium sulfate and concentrated in vacuo to an oil, which was purified using silica gel chromatography (1/2 to 2/1 ether/hexanes) to afford 22 mg (73%) of N-(3-fluoropropyl)-2β-carbomethoxy-3β-(4-chlorophenyl)nortropane as an off-white solid.

FECT. A solution of 20 mg (0.076 mmole) of 2β-carbomethoxy-3β-(4-chlorophenyl)nortropane in 5 ml of CH_2Cl_2 and 0.1 ml DMF was treated with 50 ml of Et_3N and 150 mg of 2-fluoro-1-bromoethane and stirred for 16 hr. The solution was diluted with 10 ml CH_2Cl_2, washed with 1 N NaOH, dried with sodium sulfate and concentrated in vacuo to an oil, which was purified using silica gel chromatography (1/2 to 2/1 ether/hexanes) to afford 15 mg (65%) of *N*-(2-fluoroethyl)-2β-carbomethoxy-3β-(4-chlorophenyl)nortropane as an off-white solid.

N-(3-[^{18}F]Fluoropropyl)-2β-Carbomethoxy-3β-(4-Chlorophenyl)Nortropane ([^{18}F]-4). Approximately 350 mg of ^{18}O-water containing 430 mCi of NCA ^{18}F was delivered to a vial inside a remotely-controlled robotic chemistry unit. To this vial was added 1 ml of a solution containing 10 mg K-222 (Kyrptofix), 1 mg potassium carbonate, 0.05 ml water and 0.95 ml MeCN. The solution was heated at 116°C for 3.5 min after which an additional portion of 3 ml MeCN was added and evaporated 7 min to dry the fluoride. The vial was cooled to room temperature and 2.2 mg of 1,3-diiodopropane (freshly distilled, 80°C at ~0.3 mm Hg) dissolved in 1.5 ml MeCN. The solution was heated to 82°C for 6 min, cooled to room temperature and passed through a Waters classic SiO_2 Sep-Pak into a Wheaton 5-ml microvial. The Sep-Pak was rinsed with an additional portion of MeCN, which was added to the microvial, bringing the total volume to 4 ml. Half of this solution (52 mCi) was added to another Wheaton 5-ml microvial containing 5.5 mg of 2β-carbomethoxy-3β-(4-chlorophenyl)nortropane dissolved in 0.2 ml DMF. The vial was heated to 85°C for 0.75 hr, at which point the solution was concentrated in vacuo. The residue was dissolved in a minimum of 3/1/0.25% MeOH/water/triethylamine and loaded onto a reverse-phase prep column. (Waters, 25 mm × 100 mm, flow rate 6 ml/min). The fraction eluting at 31 min contained 7.6 mCi (7.3%, based on E.O.B) of the desired product. Radio-TLC (SiO_2 90:10 CH_2Cl_2:CH_3OH, Rf = 0.7) and radio-HPLC analysis (Zorbax reverse-phase C_{18}, 4.6 mm x 250 mm, 3/1/0.25% MeOH/water/triethylamine, flow rate 1 ml/min, rt = 17 min) showed these fractions to have a radiochemical purity of greater than 99% and to have a specific activity of at least 1.15 × 10^3 Ci/mmole. The fractions containing the greatest radioactivity were concentrated in vacuo, dissolved in sterile saline w/10% EtOH and filtered through a Millipore 0.2 micron filter for in vivo studies.

Animal Tissue Distribution Experiments

Radioactivity distribution was determined in tissues of male Sprague-Dawley rats (250–300 g) after intravenous administration of the radiofluorinated tropane. The animals were allowed food and water ad libitum before the course of the experiment. The rats were anesthetized with an intramuscular injection of a 0.1 ml/100 g of a 50:50 mixture of ketamine 50 mg/ml and xylazine 20 mg/ml. The radiofluorinated tropane [^{18}F]-4 (25 μCi) in 0.1 ml of 10% ethanol in 0.9% NaCl was injected directly into the femoral vein of rats under anesthesia. The animals were killed at various times postinjection by exsanguination using a cardiac puncture under anesthesia. In rats studied at 30, 60 and 120 min postinjection, the animals were placed in cages and were reanesthetized if necessary approximately 5 min prior to being killed. An abdominal incision was made and the animals were killed by exsanquination. The organs were excised, rinsed and blotted dry. The organs were weighed and the radioactivity of the contents was determined with a Packard gamma automatic counter (Model Cobra). The percent dose per organ was calculated by a comparison of decay-corrected and background-substracted tissue counts to suitably diluted aliquots of injected material. Total activities of blood and muscle were calculated under the assumption that they were 7% and 40% of the total body weight, respectively (*24*).

Regional brain distribution was obtained in male Sprague-Dawley rats (250–300 g) after intravenous administration of radiofluorinated tropane [^{18}F]-4. The cortex, striatum and cerebellum were dissected and placed in tarred test tubes. The test tubes were weighed and radioactivity was determined with an automated gamma counter. The percent dose per gram was calculated by a comparison of decay-corrected and background-substracted tissue counts with the counts of the diluted initial injected dose. The uptake ratio of each brain region was obtained by dividing the percent/gram of each region by that of the cerebellum.

Tissue Preparation

Male Sprague-Dawley rats (200–250 g) were decapitated under ether anesthesia, and the brains excised and placed in ice. Striatal and cortical tissues were dissected, pooled and homogenized in 100 volumes (wt/vol) of ice cold Tris-HCl buffer (50 m*M*, pH 7.4). The

striatal homogenates were centrifuged at 20,000 g for 20 min and the resultant pellets were rehomogenized in the same buffer and recentrifuged. The final pellets were resuspended in a buffer composed of 50 m*M* Tris buffer (pH 7.4), 120 m*M* NaCl, 5 m*M* KCl, 2 m*M* $CaCl_2$ and 1 m*M* $MgCl_2$ and kept at −20°C for the binding assay detailed below.

Binding Assays

Tissue preparations (50 μl, 40–60 μg protein) were incubated with appropriate amounts of [^{3}H]CFT, [^{3}H]citalopram, [^{3}H]desipramine and [^{125}I]RTI-55 and competitors in a total volume of 0.2 ml of the assay buffer. The assay mixture was incubated for 60 min at room temperature with stirring and the resulting samples were rapidly filtered through Whatman GF/B glass-fiber filters pretreated with 0.2% protamine base and washed with 3 × 5 ml of cold (4°C) 50 m*M* Tris-HCl buffer, pH 7.4. Nonspecific binding was obtained in the presence of 10 μ*M* (−)-cocaine. The filters were counted in a gamma counter at an efficiency of 70% for ^{125}I or in a liquid scintillation counter at an efficiency of 65% for tritium saturation binding. Scatchard and competition experiments were analyzed with the iterative nonlinear least squares curve-fitting program (*23*).

Nonhuman Primate PET Imaging

Quantitative images of regional brain radioactivity were conducted in a 12-yr-old 12.6-kg male rhesus monkey and in a 24-yr-old 6.8-kg female rhesus monkey using a Seimens 951 31 slice PET imaging system. Images were reconstructed with a Shepp-Logan filter (0.35 X Nyquist frequency), giving a resolution of 8 mm FWHM. The animals were anesthetized with a Telazol (R) (3 mg/kg) drip and maintained on a 1% isofluorane/5% oxygen mixture throughout the imaging procedure. The animals were intubated with assurance of adequate patency of airway. They were placed on a ventilator and arterial blood gases obtained throughout the study to assure physiologic levels of respiration. An arterial catheter was placed in a distal leg artery of the animal and sewn in place to assure that it did not become dislodged. The animals were placed in the tomograph and the head was immobilized with a thermoplastic face mask. A transmission scan was then obtained with a gallium source for eventual correction of emission data. Fluorine-18-FPCT was injected in the male monkey (3.3 mCi) and female monkey (6.2 mCi) in a slow bolus infusion over 30 sec. Arterial blood sampling (0.5 ml samples) was obtained at approximately 10- to 12-sec intervals with 12 samples being obtained for the first 2 min. Samples were also obtained at 3, 4, 5, 7, 10, 20, 30, 60, 90 and 120 min after tracer injection. Kinetic emission data were acquired in the male monkey using an 18-frame acquisition protocol that included six 30-sec scans, four 3-min scans, five 10-min scans and three 20-min scans, and in the female monkey using a 20-frame acquisition protocol that included six 30-sec scans, four 3-min scans, five 10-min scans, three 20-min scans and two 30-min scans running consecutively.

After the [^{18}F]FPCT imaging protocol, [^{15}O]H_2O (10 mCi) was injected and a 2-min scan was acquired for regional brain structure coregistration. Bilateral ROIs were drawn for the striatum (caudate, putamen), thalamus, temporal cortex and cerebellum. The data were displayed as both percent dose/g and absolute uptake (nCi/ml) that were normalized for the quantity of injected dose and the weight of the monkey, and for using graphical analysis techniques of Patlak (*26*). It was found that radiotracer uptake into the bound compartment cannot be considered completely irreversible. That is, the slope of the Patlak plots continues to decrease at the latest time points. Therefore, the graphical analysis includes the reverse-rate constant designated as k_b by Patlak (*26*), which reflects the rate at which bound radiotracer reenters the blood. When this constant is incorporated into the analysis, the Patlak plots are linear.

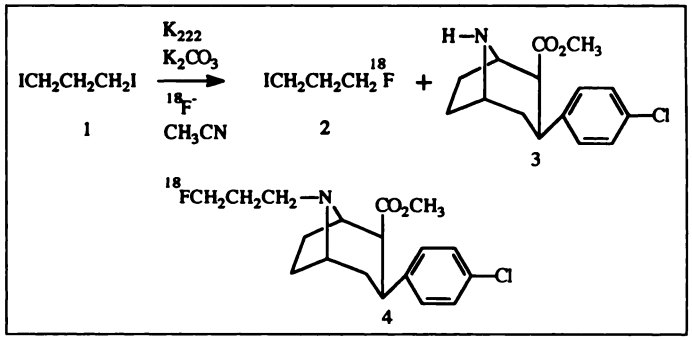

FIGURE 1. Synthesis of [^{18}F]FPCT.

Nonhuman Primate Metabolite Analysis

Arterial plasma analysis was studied in the rhesus monkeys (n = 2). Metabolite analysis was performed as described for [^{18}F]2-fluoroethylspiperone (*27*) and [^{123}I]β-CIT (*28*). Fluorine-18-FPCT was injected as described above. Arterial samples (5.0 ml) were taken at approximately 2, 5, 15, 30, 60 and 120 min after tracer injection. Plasma was extracted with ether, and the ether extracts were analyzed by radio-TLC (Whatman SiO_2, 90:10 CH_2Cl_2:CH_3OH) and radio-HPLC analysis (Waters reverse-phase C_{18}, 8 mm × 100 mm, 3/1/0.1% methanol/water/triethylamine, flow rate 1 ml/min). Extraction values for plasma samples taken at approximately 10–12-sec intervals, with 12 samples being obtained for the first 2 min and samples obtained at 4, 5, 10, 20 and 90 min after tracer injection were estimated by intermediate interpolation.

RESULTS

Chemistry

FPCT and FECT were prepared by treatment of 2β-carbomethoxy-3β-(4-chlorophenyl)nortropane (**3**) (*19*) with 1-bromo-3-fluoropropane and 1-bromo-2-fluoroethane, respectively, in refluxing acetonitrile (*29*) or in CH_2Cl_2/DMF 9/1 in the presence of triethylamine at ambient temperature. A synthetic route involving a two-step reaction sequence was developed for the no-carrier-added preparation of [^{18}F]FPCT (4). The radiosynthesis of [^{18}F]FPCT (4) used commercially available 1,3-diiodopropane (1) as the initial substrate (Fig. 1). Then 1,3-diiodopropane (1) was treated with a mixture of K_2CO_3-K222 and no-carrier-added [^{18}F]fluoride in CH_3CN at 82°C to give 1-[^{18}F]fluoro-3-iodopropane (2) in 40% yield E.O.B. Alkylation of [^{18}F]-2 with 2β-carbomethoxy-3β-(4-chlorophenyl)nortropane (**3**) in 10% DMF/CH_3CN at 85°C afforded [^{18}F]FPCT (4) in 10% overall yield E.O.B. in high-specific activity (2 Ci/μmole) in a synthesis time of 122 min.

In Vitro Binding Assays

The affinity of 8-[3-fluoropropyl]-2β-carbomethoxy-3β-(4-chlorophenyl)nortropane (4) for the dopamine transporter was determined using in vitro competitive binding assays. Competition binding data using [^{125}I]RTI-55 is shown in Table 1. The rank order of potency for binding is IPT >FPCT > FECT ≫ (−)-cocaine. The results from the binding studies demonstrate that the 8-(3-fluoropropyl) analog is four times more potent than the 8-(2-fluoroethyl) analog for competitive binding and is the preferred analog for further evaluation. Competition binding data to evaluate the selectivity of FPCT for the dopamine, and serotonin transporters using [^{3}H]CFT and [^{3}H]citalopram, respectively, is shown in Table 1. The Ki values of FPCT and CFT toward DA uptake in rat striatal homogenates are 13.8 and 40.4 n*M*, respectively, whereas Ki values toward 5-HT uptake sites in rat frontal cortical homogenates are 20.2 and 89.2 n*M*, respectively. The Ki values of FPCT and FECT toward NE uptake sites in rat frontal cortical homogenates were also

TABLE 1
Inhibition Constants (Ki, n*M*) of Various Ligands to Rat Striatal and Cortical Membranes*

Ligand	[^{125}I]RTI-55 (mean ± s.e.m.)	[^{3}H]CFT	Hill co.	[^{3}H]citalopram
IPT	3.58 ± 0.39		0.93	
CTC-iPr	7.75 ± 1.1		0.70	
FPCT	8.2 ± 0.7	13.8	1.03	20.2
FECT	32.4 ± 2.8		1.12	
CFT		40.4		89.2
(−)-cocaine	443 ± 42		0.90	

*0.3–0.5 n*M* [^{125}I]RTI-55 and 2–12 n*M* [^{3}H]citalopram were incubated in the presence of the indicated ligand in 7–11 concentrations and membrane preparation from rat striatum and cortex, respectively. Each value represents the mean ± s.e.m. of two to three determinations.

determined using [^{3}H]desipramine. The Ki values for FPCT and FECT were both found to be greater than 10,000 n*M*. These results indicate that FPCT shows no significant binding to NE transporters and is three times more potent than CFT for DA uptake sites and displays a similar 2 to 1 selectivty for DA over 5-HT uptake sites.

Tissue Distribution

The distribution of radioactivity expressed as percent dose per gram in selected tissues of 300-g male Sprague-Dawley rats at 5, 30, 60 and 120 min after femoral vein injection of 8-[3-[^{18}F]fluoropropyl]-2β-carbomethoxy-3β-(4-chlorophenyl)-nortropane is shown in Table 2. The initial level of accumulation of radioactivity in the brain after injection of [^{18}F]FPCT was high. The brain uptake exhibited a maximum at 5 min (1.27% dose/g) and exhibited a rapid global decrease at 30 min (0.48% dose/g). After 120 min the brain uptake (0.2% dose/g) had decreased by 84% when compared with the peak uptake at 5 min. In contrast to the brain, the initial blood radioactivity was low at 0.18% dose/g at 5 min. The radioactivity showed a gradual clearance from the blood. After 60 and 120 min the activity remaining in the blood decreased to 0.14 and 0.07% dose/g, respectively. The accumulation of radioactivity in the bone was initially low, 0.27% dose/g at 5 min. However, the bone radioactivity exhibited a fivefold increase to 1.33% dose/g and a sixfold increase to 1.58% dose/g at 60 and 120 min., respectively, which demonstrated moderate stability of the 3-fluoropropyl group to in vivo defluorination.

TABLE 2
Distribution of Radioactivity (% Injected Dose/g of Tissue) in Rats after Intravenous Administration of [^{18}F]FPCT*

Tissue	Time after injection; %ID dose/g (range) 5 min	30 min	60 min	120 min
Blood	0.18 (0.15–0.21)	0.21 (0.19–0.23)	0.14 (0.12–0.18)	0.07 (0.06–0.09)
Bone	0.27 (0.25–0.29)	0.65 (0.51–0.79)	1.33 (1.22–1.47)	1.58 (1.18–1.97)
Brain	1.27 (1.21–1.3)	0.71 (0.61–0.9)	0.32 (0.29–0.34)	0.16 (0.12–0.23)
Brain/Blood	7.06	3.38	2.29	2.29
Region	**5 min**	**30 min**	**60 min**	**120 min**
Striatum	1.49 (1.42–1.57)	0.92 (0.78–1.08)	0.70 (0.66–0.73)	0.38 (0.28–0.61)
Cortex	1.46 (1.39–1.52)	0.40 (0.35–0.5)	0.25 (0.21–0.32)	0.12 (0.1–0.14)
Cerebellum	0.99 (0.94–1.08)	0.24 (0.21–0.29)	0.13 (0.12–0.13)	0.06 (0.05–0.07)
Striatum/Cerebellum	1.51 (1.38–1.67)	3.94 (3.14–5.14)	5.5 (5.38–5.62)	6.2 (4.67–8.71)
Striatum/Cortex	1.03 (1.02–1.03)	2.36 (1.82–3.09)	2.82 (2.28–3.14)	3.17 (2.55–4.36)

*Mean and range values for three male Sprague-Dawley rats.

The regional distribution of radioactivity in the brain of male rats after intravenous administration of [^{18}F]FPCT is also shown in Table 2. The level of accumulation of radioactivity was high in the striatum, a brain region rich in dopamine uptake sites. The striatum showed a maximum at 5 min (1.49% dose/g) and exhibited a 39% decrease at 30 min (0.92% dose/g). After 60 and 120 min the striatum uptake decreased 47% (0.70% dose/g) and 74% (0.38% dose/g), respectively, when compared to peak striatal activity at 5 min. In contrast to the initial high uptake and gradual clearance of radioactivity in the striatum, the cerebellum and the cortex regions of low dopamine uptake site density showed a rapid washout of radioactivity. The cerebellum showed a maximum at 5 min (0.99% dose/g) and exhibited a 94% decrease at 120 min (0.06% dose/g). The cortex showed a maximum at 5 min (1.46% dose/g) and exhibited a 92% decrease at 120 min (0.12% dose/g). The striatum-to-cerebellum (ST/CB) ratio was 1.51, 3.94, 5.62 and 6.19 at 5, 30, 60 and 120 min, respectively.

PET Brain Imaging of Fluorine-18-FPCT in a Rhesus Monkey

The results of a dynamic imaging study of [^{18}F]FPCT at 12–15 min, 65–85 min, 85–105 min and 105–125 min. in the 12-yr-old male rhesus monkey is shown in Figure 2. The caudate and putamen were the areas of highest accumulation of [^{18}F]FPCT. The brain images of one plane from 105 min to 125 min demonstrate no visible accumulation of [^{18}F]FPCT in cortical regions of the brain that strongly suggests low in vivo affinity for 5-HT uptake sites in the rhesus. Time-activity curves of selected brain regions in the male and female rhesus monkey are shown in Figures 3 and 4, respectively. Radioactivity uptake (Figs. 3 and 4), as determined from ROIs of transverse and coronal projections, demonstrate that the putamen (P) and caudate (C) rapidly increased with time and remained relatively constant from 40 min (P = 0.03%–0.11% dose/g; C = 0.02%–0.08% dose/g) to 115 min (P = 0.03%–0.12% dose/g; C = 0.02%–0.08% dose/g). Radioactivity uptake in the cerebellum peaked at 13.5 min (0.02%–0.09% dose/g), then rapidly decreased with time, falling to 0.01%–0.05% dose/g at 75 min and to 0.01%–0.04% dose/g at 115 min. At 115 min, the radioactivity in the cerebellum appeared to be still decreasing. The ratio of caudate and putamen-to-cerebellum tissue radioactivity were 2.27–2.29 and 3.34–3.36, respectively, at 115 min. Radioactivity uptake, as measured from transaxial projections, in the cortex peaked at 30 min (0.012%–0.044% dose/g), then rapidly decreased with time, falling to 0.01%–0.037% dose/g at 115 min. At 115 min, the radioactivity in the cortex appeared to be still decreasing. The ratio of putamen-to-cortex tissue radioactivity was 3.19–3.31 at 115 min. Graphical analysis techniques (Patlak plots) for five regions of the rhesus monkey brains are shown in Figures 5 and 6. The arterial plasma data were corrected for metabolites. Because the metabolite analysis indicated no significant lipophilic metabolites, no correction for metabolites was applied to the image data. The influx rate constants, K_1 (1/sec), for the

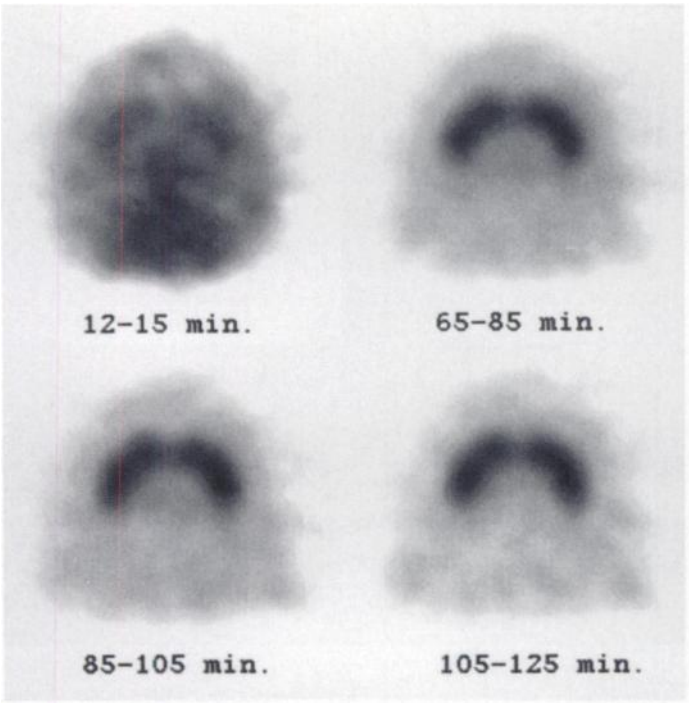

FIGURE 2. Transaxial brain images of a single-plane image of [^{18}F]FPCT at 12–15 min, 65–85 min, 85–105 min and 105–125 min in a male rhesus monkey.

12-yr-old male monkey (Fig. 5), as determined from the slope of the later portion of the plots, are: putamen 0.0075, caudate 0.0055, thalamus 0.0045, temporal cortex 0.0028 and cerebellum 0.0024. The influx rate constants, K_1 (1/sec), for the 24-yr-old female monkey (Fig. 6), as determined from the slope of the later portion of the plots, are: putamen 0.0023, caudate 0.0017, thalamus 0.0011, temporal cortex 0.0005 and cerebellum 0.00023. The reverse-rate constants, Kb (1/sec), describing the bound activity returning to the blood, were very small, indicating that the tracer is essentially irreversibly trapped in the transporter for the duration of the study.

Pharmacokinetic Studies

Rhesus (n = 2) arterial plasma samples were analyzed for metabolites by an extraction method (*28*) after femoral vein injection of [^{18}F]FPCT. The major initial arterial plasma radiolabeled component was ether extractable and displayed a single peak (>99% pure), both TLC and HPLC analysis, which corresponded to unmetabolized authentic FPCT. The fraction of unmetabolized [^{18}F]FPCT in arterial plasma rapidly decreased from 87% at 2–3 min to 31% at 14–16 min. (Table 3). The major arterial plasma radiolabeled metabolite was a polar nonextractable component, which increased to 96% of the plasma activity by 120 min. The arterial input function of [^{18}F]FPCT in the rhesus (n = 2) monkeys is shown in Figure 7. After slow bolus (30-sec) intravenous administration of [^{18}F]FPCT, peak arterial plasma ^{18}F radioactivity was reached at 2.4 min. The arterial plasma fraction of unmetabolized [^{18}F]FPCT had a $T_{1/2}$ = 78 min.

DISCUSSION

We obtained successful no-carrier-added radiofluorination with K^{18}F and evaluation of FPCT as a potential PET radioligand for mapping CNS dopamine uptake sites. FPCT is an analog of a series of 2β-carbomethoxy-3β-(4-substituted phenyl)tropanes that are high affinity ligands for the dopamine transporter in which the 8-methyl substituent has been replaced by a 3-[^{18}F]fluoropropyl group. The 4-chloro- derivative, 2β-carbomethoxy-3β-(4-chlorophenyl)tropane, was reported to be one of the most potent members of the series, exhibiting low nanomolar potency (IC_{50}=1.17 n*M*) for the dopamine transporter from competition binding with rat striatal tissue preparation for [^{3}H]-2β-carbomethoxy- 3β-(4-fluorophenyl)tropane, CFT (1). In vivo imaging studies of dopamine reuptake sites in nonhuman primates with radioiodinated [^{123}I]IPT (*30*), has also recently been reported.

We reported, in a preliminary communication, the radiosynthesis of [^{18}F]FPCT by a two-step reaction sequence that first involved the preparation of 1-bromo-3-[^{18}F]fluoropropane from 1-bromo-3-trifluoromethanesulfonyloxypropane followed by alkylation of 2β-carbomethoxy-3β-(4-chlorophenyl)nortro-

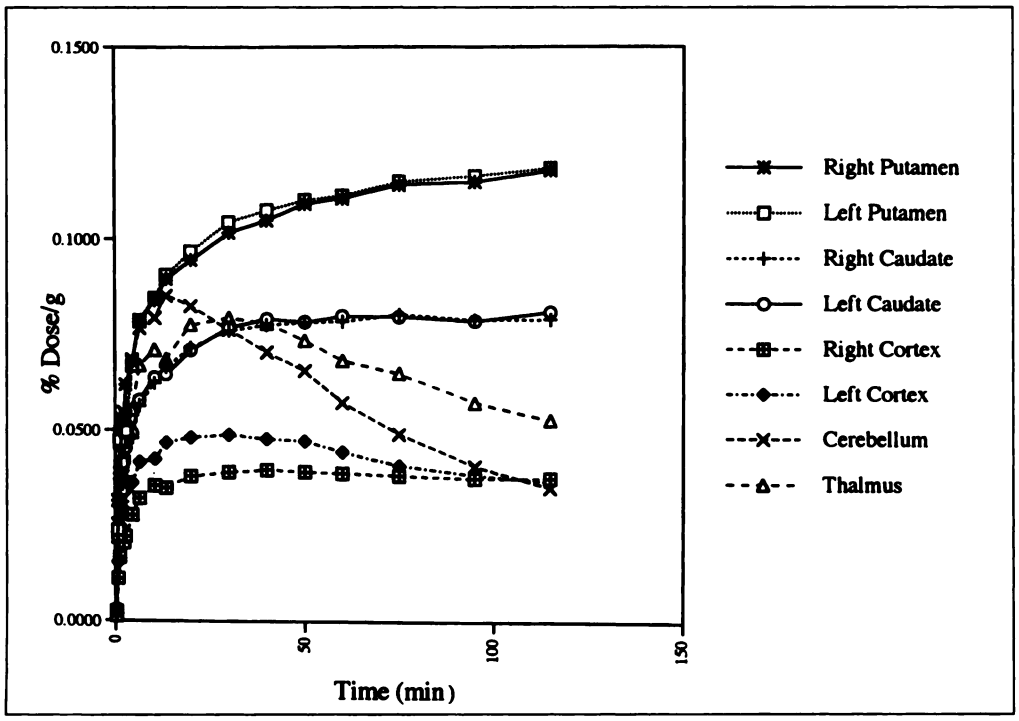

FIGURE 3. Time-activity curves in various regions of a male rhesus monkey's brain recieving 3.3 mCi of [^{18}F]FPCT. Serial images were acquired for a total time of 125 min (18 scans).

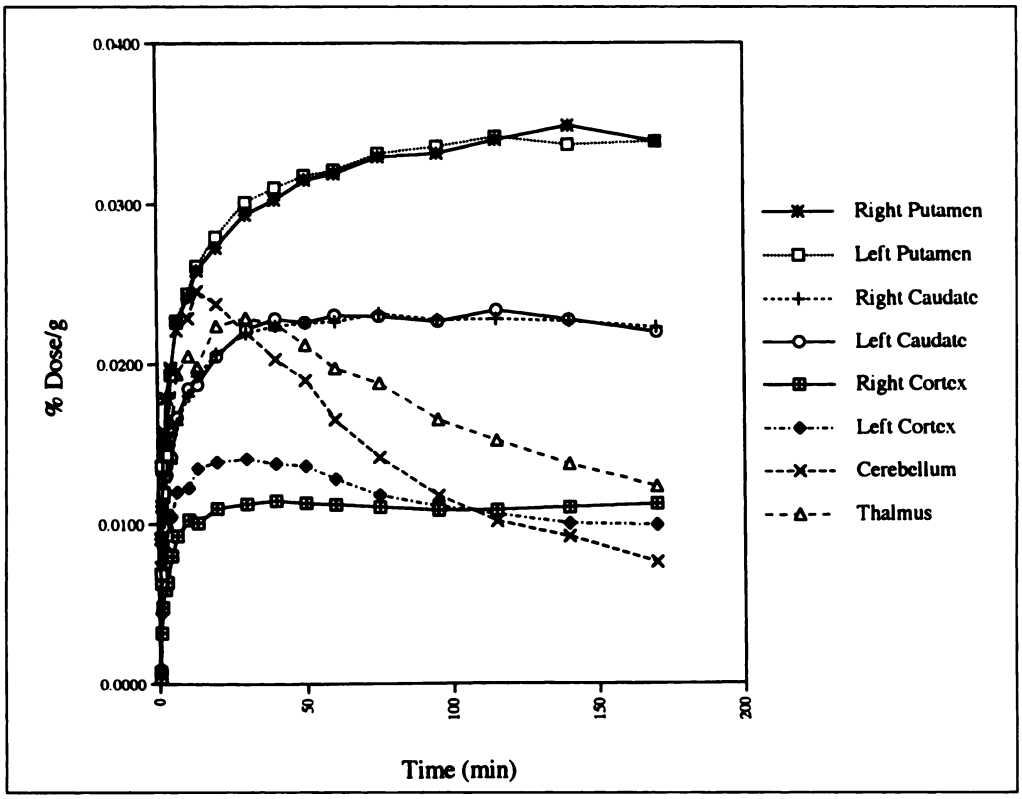

FIGURE 4. Time-activity curves in various regions of a male rhesus monkey's brain recieving 6.2 mCi [^{18}F]FPCT. Serial images were acquired for a total time of 185 min (20 scans).

pane (*29*). The first step in the reaction sequence was not reproducible on a routine basis and required fresh preparation of 1-bromo-3-trifluoromethanesulfonyloxypropane. Analysis of the reaction mixture of 1-bromo-3-trifluoromethanesulfonyloxypropane with K^{18}F/K222 in CH_3CN at 85°C by radio-TLC indicated formation of significant amounts of 1-[^{18}F]fluoro-3-trifluoromethanesulfonyloxypropane in addition to the desired 1-bromo-3-[^{18}F]fluoropropane. Treatment of 2β-carbomethoxy-3β-(4-chlorophenyl)nortropane with 1-[^{18}F]fluoro-3-trifluoromethanesulfonyloxypropane in CH_3CN at 85°C does not result in [^{18}F]FPCT (4), thus lowering the overall yield. We have developed an improved method for the preparation of [^{18}F]FPCT (4) (Fig. 1), using commercially available 1,3-diiodopropane (1) as the initial substrate. 1,3-diiodopropane (1) was treated with NCA K[^{18}F]/K222 to give 1-[^{18}F]fluoro-3-iodopropane (2). Coupling of [^{18}F]2 with 2β-carbomethoxy-3β-(4-chlorophenyl)nortropane (3) afforded [^{18}F]FPCT (4) in 65% yield (based upon [^{18}F] 2) E.O.S. [^{18}F]FPCT (4) was purified on a large Waters semiprep C_{18} RP 25-mm X 100-mm column in order to efficiently separate [^{18}F]FPCT, 10% radiochemical yield E.O.B., from the major labeled and unlabeled side products, 1-[^{18}F]fluoro-3-iodopropane (2) and 8-[3-iodopropyl]-2β-carbomethoxy-3β-(4-chlorophenyl)nortropane, respectively.

In vitro displacement studies with rat tissue preparations showed that FPCT was a potent inhibitor of dopamine uptake at the transporter. FPCT exhibited its most potent displacement, at nanomolar levels, for the dopamine transporter ligands [^{3}H]CFT and [^{125}I]β-CIT in rat striatal tissue. Moderate selectivity of FPCT was demonstrated in the in vitro competitive binding experiment with the serotonin transporter ligand

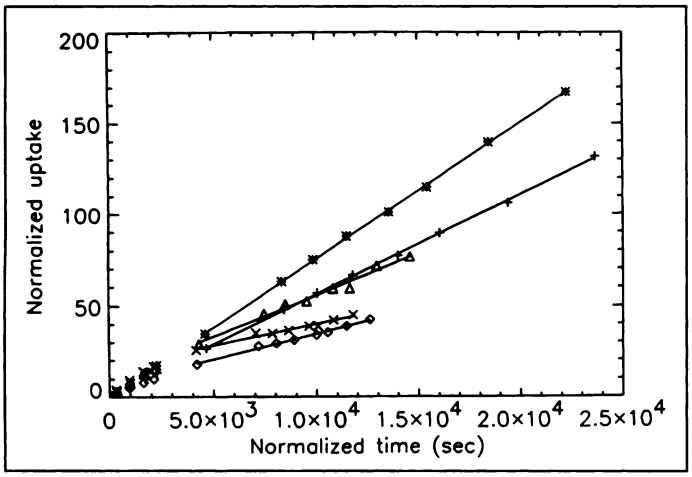

FIGURE 5. Patlak graphical analysis for average of left and right putamen (*), average of left and right caudate (+), average of left and right cortex (◇), thalmus (△) and cerebellum (X) brain regions of the male rhesus monkey. Scans were acquired continuously for 125 min.

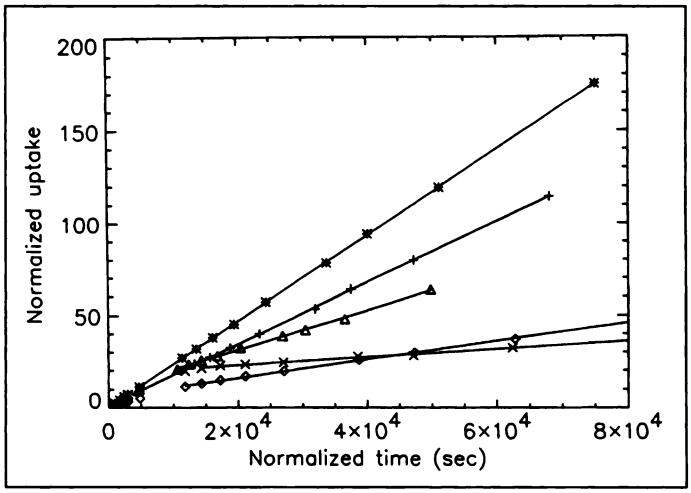

FIGURE 6. Patlak graphical analysis for average of left and right putamen (*), average of left and right caudate (+), average of left and right cortex (◇), thalmus (△) and cerebellum (X) brain regions of the female rhesus monkey. Scans were acquired continuously for 185 min.

TABLE 3
Percent Composition and Metabolite Analysis of Rhesus Monkey Blood after Intravenous Injection of Fluorine-18-FPCT (Average of Two Animals)

Time (min)	% Aqueos	% Ether	% [^{18}F]FPCT Ether
2–3	13	87	99
5–7	34	66	99
14–16	69	31	99
30	88	12	99
60	93	7	99
120	96	4	99

[^{3}H]citalopram in rat cortical tissue. FPCT showed a twofold higher selectivity for the dopamine transporter over the serotonin transporter.

The selectivity of FPCT for the dopamine transporter was more clearly demonstrated in the in vivo studies. In the in vivo tissue distribiution in rats, FPCT showed high uptake and good retention in the striatum, a brain region of high dopamine transporter density. In contrast, FPCT showed rapid washout from rat cerebellum and cortical tissue which are regions of low dopamine transporter density and high serotonin transporter density, respectively. FPCT showed high striatal to cerebellum ratios, 6 to 1, and good striatal to cortical ratios 3 to 1 at 2 hr postinjection. The absence of retention of FPCT for cortical tissue in the in vivo studies suggests that FPCT is a selective dopamine transporter ligand. These results are similar to those for the radioiodinated N-substituted alkenyl derivative, 8-[(E)-3-[^{123}I]iodopropen-1-yl] substitution of 2β-carbomethoxy-3β-(4-chlorophenyl)nortropane (IPT) that we recently developed (*23,31*). In our earlier studies we demonstrated that 8-[(E)-3-[^{123}I]iodopropen-1-yl] 2β-carbomethoxy-3β-(4-chlorophenyl) tropane exhibited high striatal to cerebellum ratios (16.5 at 2 hr) and high striatal to cortical ratios (12 at 2 hr), even though the specific binding of [^{125}I]IPT in rat cortical tissue was inhibited by paroxetine, a potent serotonin transporter ligand, at Ki = 0.5 n*M*.

The in vivo selectivity of FPCT for the dopamine transporter rich striatum was further demonstrated in in vivo nonhuman primate imaging. Rapid and pronounced accumulation of radioactivity with long retention was visualized in the striatum of the rhesus monkey. The localization of radioactivity was absent in both the dopamine transporter poor cerebellum and cortical regions. Time-activity measurements of brain regions of the rhesus monkey corroborated the high imaging signal seen in the striatum. Striatum-to-cerebellum and striatum-to-cortex ratios were 3–3.3 from 105–125 min postinjection. The imaging results for FPCT are characteristic for a potent and selective dopamine transporter imaging agent.

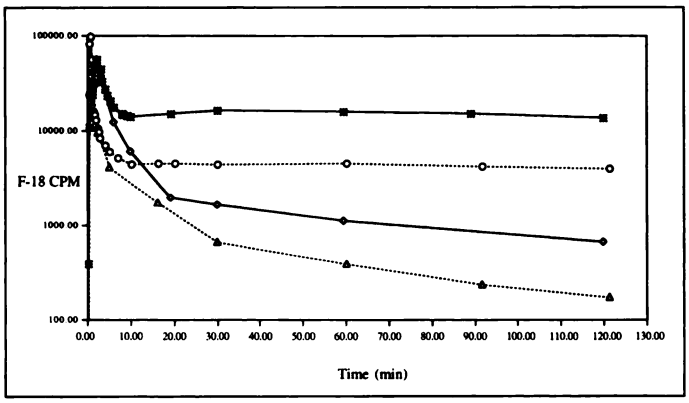

FIGURE 7. Arterial input function for [^{18}F]FPCT in a male and a female rhesus monkey. Total arterial ^{18}F plasma activity in the male monkey (*), total arterial ^{18}F plasma activity in the female monkey (○), arterial parent [^{18}F]FPCT activity in the male monkey (◇) and arterial parent [^{18}F]FPCT activity in the female monkey (△).

The selectivity of FPCT for the dopamine transporter is further demonstrated by graphical analysis (Patlak) techniques. The influx rate constant (K_1) for the thalamus is clearly above the background and below the basal ganglia levels. Visualization of dopamine transporters in the thalamus is consistent with the existence of dopamine D2 receptors seen in the thalamus of the postmortem human brain (*32*). The identical nature of the cortex and cerebellar curves indicates that there is very little, if any, nonspecific binding of FPCT in the brain (Figs. 5 and 6). The similar clearance rates for the parent compound in the plasma (Fig. 7) and the cerebellum (Figs. 3 and 4) indicate that the nondopamine-rich tissues are in rapid equilibrium with FPCT in the plasma. Therefore, FPCT appears to be a very specific ligand for dopamine transporters with good imaging characteristics.

The analysis of labeled metabolites in the arterial plasma of the rhesus monkey, after intravenous injection by ether extraction and radio-TLC and radio-HPLC analyses, showed the rapid appearance of one major hydrophilic metabolite at 14 min postinjection. The identity of the polar metabolite was not elucidated. The remaining fraction of radioactivity in the arterial plasma was identified as unmetabolized FPCT. The absence of labeled lipophilic metabolites in the arterial plasma that could reenter the brain permits calculation of the [^{18}F]FPCT input function and subsequent quantification of binding sites.

CONCLUSION

A no-carrier-added radiosynthesis has been developed for [^{18}F]FPCT. Preliminary in vivo imaging studies revealed that FPCT showed high affinity for the dopamine transporter. In vivo tissue distribution studies in rats and nonhuman primate imaging studies demonstrated pronounced striatal uptake and retention, rapid clearance from cerebellum and cortical brain regions, and the absence of the accumulation of lipophilic metabolites in plasma. These results suggest that [^{18}F]FPCT is an excellent candidate for further evaluation for mapping dopamine transporters in humans in conjunction with PET.

APPENDIX

Spectroscopic and microanalytical characterization of N-(3-fluoropropyl)-2β-carbomethoxy-3β-(4-chlorophenyl)nortropane, 4.

^{1}H NMR (300 MHz, $CDCl_3$): δ 7.21 (m, 4H, Ar-H), δ 4.51 (dt, 2H, αF-CH_2, J = 41 Hz, 5.7Hz,), δ 3.68 (m, 1H, H-1), δ 3.48 (s, 3H, OCH_3), δ 3.40 (m, 1H, H-5), d 2.96 (dd, 1H, H-3), δ 2.90 (t, 1H, H-2), δ 2.54 (t, 1H, H-4_{ax}), δ 2.37 (m, 2H, αN-CH_2), δ 2.05 (m, 2H), d 1.58–1.77 (m, 3H); ^{13}C NMR (75 MHz, $CDCl_3$): δ 171.74 (CO_2Me), δ 141.71 (Ar), δ 131.405 (Ar), δ 128.62 (Ar), δ 127.94 (Ar), δ 82.1 (d, αF-C, J = 198 Hz), δ 63.18 (C-1), δ 61.37 (C-5), δ 52.75 (COCH3), δ 50.909 (C-2), δ 49.26 (d, γF-C, J = 62 Hz), δ 34.01(C-3), δ 33.73 (C-4), δ 29.95 (d, βF-C, J = 20 Hz), δ 25.90 (C-6), δ 25.99 (C-7); LRMS (E.I.) (m/z 339, (M^+, 18%)); HRMS (E.I.): for $C_{18}H_{23}ClFO_2N$: calc. 339.1431, found: 339.1401; Anal. C, H, N.

Spectroscopic and microanalytical characterization of *N*-(2-fluoroethyl)-2β-carbomethoxy-3β-(4-chlorophenyl)nortropane.

^{1}H NMR (300 MHz, $CDCl_3$): δ 7.21 (m, 4H, Ar-H), δ 4.45 (m, 2H, αF-CH_2), δ 3.79 (m, 1H, H-1), δ 3.51 (s, 3H, OCH_3), δ 3.45 (m, 1H, H-5), δ 2.96 (dd, 1H, H-3), δ 2.90 (t, 1H, H-2), δ 2.62–2.53 (m, 3H, H-4_{ax} & αN-CH_2), δ 1.99–2.15 (m, 2H), δ 1.58–1.77 (m,

3H); LRMS (E.I.) (m/z 325, (M^+, 2%)); HRMS (E.I.): for $C_{17}H_{21}ClFO_2N$: calc. 325.1135, found: 339.1245; Anal. C, H, N.

ACKNOWLEDGMENTS

This research was sponsored by the Office of Health and Environmental Research, U.S. Department of Energy under grant number DE-FG05-93ER61737 and the National Institute of Mental Health Drug Screening Program. We thank Marinell Barber for assistance in preparing the manuscript and Justin Baker for assistance in data analysis.

REFERENCES

1. Carroll FI, Lewin AH, Boja JW, Kuhar MJ. Cocaine receptor: biochemical characterization and structure-activity relationships of cocaine analogues at the dopamine transporter. *J Med Chem* 1992;35:969–981.
2. Kaufman MJ, Madras BK. Severe depletion of cocaine recognition sites associated with the dopamine transporter in Parkinson's diseased striatum. *Synapse* 1991;49:43–49.
3. Bernheimer H, Birkmayer W, Hornykiewcz O, et al. Brain dopamine and the syndromes of Parkinson and Huntington: clinical, morphological and neurochemical correlations. *J Neurol Sci* 1973;20:415–455.
4. Brooks DJ, Playford ED, Ibanez V, et al. Isolated tremor and disruption of the nigrostriatal dopaminergic system: an ^{18}F-dopa PET study. *Neurology* 1992;42:1554–1560.
5. Niznik HB, Fogel EF, Fassos EF, Seeman P. The dopamine transporter is absent in Parkinson's putamen and reduced in the caudate nucleus. *J Neurochem* 1991;56:192–198.
6. Fowler J S, Volkow ND, Wolf AP, et al. Mapping cocaine binding sites in human and baboon brain in vivo. *Synapse* 1989;4:371–377.
7. Logan J, Fowler J S, Volkow ND, et al. Graphical analysis of reversible radioligand binding from time-activity measurements applied to [N-^{11}C-methyl]-(−)-cocaine pet studies in human subjects. *J Cereb Blood Flow Metab* 1990;5:740–747.
8. Yu D-W, Macgregor RR, Wolf AP, Fowler J S, Dewey S L, Schlyer DJ. Halogenated cocaine analogs for PET and SPECT studies. *J Labelled Comp Radiopharm* 1991;30:394–396.
9. Yu D-W, Gatley SJ, Wolf AP, et al. Synthesis of carbon-11 labeled iodinated cocaine derivatives and their distribution in baboon brain measured using positron emission tomography. *J Med Chem* 1992;35:2178–2183.
10. Aquilonius S M, Bergstrom K, Eckernas SA, et al. In vivo evaluation of striatal dopamine reuptake sites using ^{11}C-nomifensine and positron emission tomography. *Acta Neurol Scand* 1987;76:283–287.
11. Kilbourn MR, Haka MS. Synthesis of [^{18}F]GBR 13119. A presynaptic dopamine uptake antagonist. *Appl Radiat Isot* 1988;39:279–282.
12. Kilbourn MR. In vivo binding of [^{18}F]GBR 13119 to the brain dopamine uptake system. *Life Sci* 1988;42:1347–1353.
13. Kilbourn MR, Carey JE, Koeppe RA, et al. Biodistribution, dosimetry, metabolism and monkey PET studies of [^{18}F]GBR 13119. Imaging the dopamine uptake system in vivo. *Nucl Med Biol* 1989;16:569–576.
14. Carroll FI, Gao Y, Rahman MA, et al. Synthesis, ligand binding, QSAR, CoMFA study of 3β-(p-substituted phenyl)tropane-2β-carboxylic acid methyl esters. *J Med Chem* 1991;34:2719–2725.
15. Frost JJ, Rosier AJ, Reich SG, et al. Positron emission tomographic imaging of the dopamine transporter with ^{11}C-WIN 35,428 reveals marked declines in mild Parkinson's disease. *Ann Neurol* 1993;34:423–431.
16. Meltzer PC, Liang AY, Brownell AL, Elmaleh DR, Madras BK. Substituted 3-phenyltropane analogs of cocaine: synthesis, inhibition of binding at cocaine recognition sites and positron emission tomography imaging. *J Med Chem* 1993;36:855–862.
17. Dannals RF, Neumeyer JL, Milius RA, Ravert HT, Wilson AA, Wagner Jr HN. Synthesis of a radiotracer for studying dopamine uptake site in vivo using PET: 2β-carbomethoxy-3β-(p-fluorophenyl)-[N-^{11}C-methyl]tropane ([^{11}C]CFT or (^{11}C-WIN 35,428). *J Labeled Comp Radiopharm* 1993;33:147–152.
18. Muller L, Halldin C, Farde L, et al. [^{11}C]B-CIT, a cocaine analogue. Preparation, autoradiography and preliminary PET investigations. *Nucl Med Biol* 1993;20:249–255.
19. Carroll FI, Rahman MA, Abraham P, et al. Iodine-123-3β-(4-iodophenyl)tropan-2β-carboxylic acid methyl ester (RTI-55). A unique cocaine receptor ligand for imaging the dopamine and serotonin transporters in vivo. *Med Chem Res* 1991;1:289–294.
20. Neumeyer JL, Wang S, Milius RA, et al. Iodine-123-2β-carbomethoxy-3β-(4-iodophenyl)tropane: high affinity SPECT radiotracer of monoamine reuptake sites in brain. *J Med Chem* 1991;34:3144–3146.
21. Innis RB, Baldwin RM, Sysbirska E, et al. Single photon emission computed tomography imaging of monoamine reuptake sites in primate brain with [^{123}I]CIT. *Eur J Pharmacol* 1991;200:369–370.
22. Shaya E, Scheffel U, Dannals RH, et al. In vivo imaging of dopamine reuptake sites in the primate brain using SPECT and iodine-123-labeled RTI-55. *Synapse* 1992;10:169–172.
23. Goodman MM, Kung MP, Kabalka GW, Kung HF, Switzer R. Synthesis and characterization of radioiodinated N-(3-iodopropen-1-yl)-2β-carbomethoxy-3β-(4-chlorophenyl)-tropanes: potential dopamine reuptake site imaging agents. *J Med Chem* 1994;37:1535–1542.
24. Zamora PO, Eshima D, Graham D, Shattuck L, Rhodes BA. Biological distribution of ^{99m}Tc-labeled YIGSR and IKVAV laminin peptides in rodents: ^{99m}Tc-IKVAV peptides localizes to the lung. *Biochem Biophys Acta* 1993;00:1–8.
25. Mailson RT, Vessotskie, Kung MP, et al. SPECT imaging of striatal dopamine transporters in nonhuman primates with N-(3-iodopropen-1-yl)-2β-carbomethoxy-3β-(4-chlorophenyl)-tropane ([^{123}I]IPT). *J Nucl Med* 1995;36:2290–2297.
26. Patlak CS, Blasberg RG. Graphical evaluation of blood-to-brain transfer constant from multiple-time uptake data generalizations. *J Cereb Blood Flow and Metab* 1985;5:584–590.
27. Barrio J, Satyamurthy N, Huang A, et al. 3-(2'-[^{18}F]fluoroethyl)spiperone: in vivo biochemical and kinetic characterization in rodents, nonhuman primates and humans. *J Cereb Blood Flow Metab* 1989;6:830–839.
28. Baldwin RM, Zea-Ponce Y, Zoghbi S, et al. Evaluation of the monoamine uptake site ligand ([^{123}I]β-CIT) in nonhuman primates: pharmacokinetics, biodistribution and SPECT brain imaging coregistered with MRI. *Nucl Med Biol* 1993;20:597–606.
29. Goodman MM, Kabalka GW, Kung MP, Kung HF, Meyer MA, Synthesis of [^{18}F]-N-3-fluoropropyl-2β-carbomethoxy-3β-4-chlorophenyl)tropane. A high affinity neuroligand to map dopamine uptake sites by PET. *J Labeled Comp Radiopharm* 1994;34:488–490.
30. Neumeyer JL, Wang S, Gao Y, et al. N-ω-fluoroalkyl analogs of (1R)-2-β-cabomethoxy-3-β(4-iodophenyl)tropane (β-CIT): radiotracers for PET and SPECT imaging of dopamine transporters. *J Med Chem* 1994;37:1558–1561.
31. Kung MP, Essman WD, Frederick D, et al. A novel iodinated ligand for the CNS dopamine transporter. *Synapse* 1995;20:316–324.
32. Kessler RM, Whetsell WO, Ansari MS, et al. Identification of extrastriatal dopamine D2 receptors in postmortem human brain with [^{125}I]epidepride. *Brain Res* 1993;609:237–243.